BIOCHEMISTRY
including biophysical chemistry & molecular biology

Article

McbR/YncC: implications for the mechanism of ligand and DNA binding by a bacterial GntR transcriptional regulator involved in biofilm formation

Dana M Lord, AY#E UZGÖREN BARAN, Valerie W. C. Soo,
Thomas Keith Wood, Wolfgang Peti, and Rebecca Page

Biochemistry, **Just Accepted Manuscript** • DOI: 10.1021/bi500871a • Publication Date (Web): 23 Oct 2014

Just Accepted

Biochemistry is published by the American Chemical Society. 1155 Sixteenth Street N.W., Washington, DC 20036

McbR/YncC: implications for the mechanism of ligand and DNA binding by a bacterial GntR transcriptional regulator involved in biofilm formation

Dana M. Lord,[1,2] Ayse Uzgoren Baran,[3,5] Valerie W. C. Soo,[4] Thomas K. Wood,[4] Wolfgang Peti[3] and Rebecca Page[1,]*

[1]Department of Molecular Biology, Cell Biology and Biochemistry, [2]Graduate Program in Molecular Pharmacology and Physiology and [3]Department of Molecular Pharmacology, Physiology and Biotechnology & Chemistry, Brown University, Providence, Rhode Island 02903, United States, [4]Departments of Chemical Engineering & Biochemistry and Molecular Biology, Pennsylvania State University, University Park, PA 16802; [5]*Current address*: Department of Chemistry, Hacettepe University, Faculty of Science, Beytepe, 06800 Ankara-Turkey.

Funding Sources

This work was supported by a National Science Foundation-Experimental Program to Stimulate Competitive Research (EPSCoR Grant No. 1004057) graduate fellowship to DML, an Army

Research Office award to TKW (W911NF-14-1-079) and a National Science Foundation-CAREER Award MCB-0952550 to RP.

Corresponding Author

*Email: rebecca_page@brown.edu Phone: 401-863-6076 Fax: 401-863-9653

ABBREVIATIONS

ASU, asymmetric unit; CD, circular dichroism; EPS, exopolysaccharide; EDTA, ethylenediaminetetraacetic acid; EMSA, electrophoretic mobility shift assay; FCD, FadR C-terminal domain; IPTG, isopropyl-beta-D-thiogalactopyranoside; MPD, 2-Methyl-2,4-pentanediol; PDB, protein data bank; SEC, size exclusion chromatography; SeMet, selenomethionine; TCEP, Tris(2-carboxyethyl)phosphine; TEV, Tobacco Etch Virus; wHTH, winged helix-turn-helix; WT, wild-type

ABSTRACT

MqsR-controlled colanic acid and biofilm regulator (McbR, also known as YncC) is the protein product of a highly induced gene in early *E. coli* biofilm development and has been regarded as an attractive target for blocking biofilm formation. This protein acts as a repressor for genes involved in exopolysaccharide production and an activator for genes involved in the stress response. To better understand the role of McbR in governing the switch from exponential growth to the biofilm state, we determined the crystal structure of McbR to 2.1 Å. The structure reveals McbR to be a member of the FadR C-terminal domain (FCD) family of the GntR superfamily of transcriptional regulators (this family was named after the first identified member, GntR, a transcriptional repressor of the gluconate operon of *Bacillus subtilis*). Previous to this study, only six of the predicted 2800 members of this family had been structurally characterized. Here we identify the residues that constitute the McbR effector and DNA binding sites. In addition, comparison of McbR with other members of the FCD domain family shows that this family of proteins adopts highly distinct oligomerization interfaces, which has implications for DNA binding and regulation.

Biofilms are complex communities of bacteria that are encased in an extracellular matrix and adhere to almost any surface. Due to properties of the biofilm, these bacterial communities are extremely tolerant to antibiotics and are often able to evade host defenses.[1] Furthermore, it is estimated that 60-80% of human infections are caused by biofilms, explaining why much research is focused on elucidating the genetic basis of biofilm formation and proliferation.[2, 3] One regulator of biofilm formation is McbR/YncC (hereafter referred to as McbR), a transcription factor predicted to belong to the GntR family of DNA binding proteins. In *E. coli*, deletion of *mcbR* results in the overproduction of colanic acid,[4] a constituent of the biofilm exopolysaccharide (EPS) matrix composed of glucose, galactose, fucose, and glucuronic acid in the ratio 1:2:2:1.[5] As a consequence, *mcbR* deletion results in a mucoidy phenotype and a reduction in biofilm formation. In *E. coli*, gene array studies coupled with electrophoretic mobility shift assays (EMSAs) showed that McbR binds the *ybiM* promoter, a gene encoding a putative periplasmic protein whose function is currently unknown.[4] A subsequent study using DNA footprinting experiments showed that McbR from *S. typhimurium* and *E. coli* binds the *yciG* promoters from both species.[6]

The GntR superfamily (Pfam PF00392), to which McbR belongs, is one of the largest families of transcriptional regulators with more than 8500 members (**Fig. 1A**).[7] Members of this family contain an N-terminal DNA-binding winged helix-turn-helix (wHTH) domain and a C-terminal effector-binding/oligomerization domain. In contrast to the wHTH domain, which is structurally conserved in the GntR family, the C-terminal domain is highly variable. Detailed bioinformatics studies have led to the definition of at least 7 families (AraR, DevA, FCD, HutC, MocR, PlmA and YtrA), which are classified by the effector-binding domain topology and secondary structure (**Fig. 1A**).[7] The majority of GntR regulators belong to the FadR C-terminal

domain family (FCD, Pfam PF07729; **Fig. 1A**). The effector molecule which regulates the activity of GntR transcriptional regulators is often a product/substrate in the metabolic pathway that the particular GntR transcription factor controls. However, there are examples where this is not the case and difficulties in identifying the endogenous ligands for this family have limited our understanding of how these regulators function *in vivo*.[7] What is known is that effector binding in the C-terminal effector binding domains alter, via poorly understood structural mechanism(s), the conformations and/or relative orientations of the N-terminal wHTH domains. This, in turn, inhibits DNA binding.[7] This limited understanding is due to the dearth of structural data available for the GntR superfamily, especially those of the FCD family. Here, we describe the structure of McbR from *E. coli* to 2.1 Å resolution. We show that McbR belongs to the FCD-family of transcriptional regulators and identify the residues that mediate DNA binding. We also identify the residues that constitute its effector binding site, which are highly conserved in *mcbR* homologues. Finally, a comparison of the currently available structures of FCD transcriptional regulators reveals different oligomerization interfaces at the wHTH domains,[8-10] suggesting this family of proteins undergoes distinct conformational rearrangements upon ligand binding.

MATERIALS AND METHODS

Protein expression and purification.

Two constructs of wild-type McbR ($McbR_{1-221}$ (full-length), residues 1-221; $McbR_{10-221}$, residues 10-221) were sub-cloned into the pRP1B bacterial expression vector, which contains an N-terminal His_6-tag and Tobacco Etch Virus (TEV) cleavage site;[11] both constructs were sequenced prior to subsequent experiments. pRP1B-$McbR_{1-221}$ variants (single mutant variants:

Arg34Ala, Lys38Ala, Thr49Ala, Arg52Ala, Gln70Ala; double mutant variant: Glu93Ser/Arg139Phe; triple mutant variant: Arg89Ala/Glu93Ala/Arg139Ala) were generated using the QuikChange Mutagenesis Kit (Agilent Technologies) using the manufacturer's protocols; all constructs were verified by sequencing.

WT McbR and McbR variants were expressed in *E. coli* BL21-Gold (DE3) cells (Agilent). Cells were grown at 37°C (250 rpm) to an OD_{600} of ~0.9, at which point the cells were transferred to 4ºC for 1 hour. The cells were induced with 0.5 mM IPTG and grown overnight at 18ºC (250rpm). The cells were then harvested by centrifugation at 6,000 ×g. Selenomethionine (SeMet)-labeled $McbR_{10\text{-}221}$ was produced using identical protocols, with the exception that the cells were grown in minimal medium supplemented with vitamins, metals and amino acids (with selenomethionine substituted for methionine).[12]

For purification, cell pellets of either WT McbR or McbR variants were resuspended in lysis buffer (50 mM Tris pH 8.0, 500 mM NaCl, 0.1% Triton X-100, 5 mM imidazole, Complete tabs-EDTA free [Roche]) and lysed by high-pressure homogenization (C3 Emulsiflex; Avestin). Following centrifugation (45,000 ×g/45 min/4°C), the supernatant was applied to a HisTrap HP column (GE Healthcare) and McbR eluted using a 5-500 mM imidazole gradient. McbR was then incubated overnight with TEV protease (50 mM Tris pH 8.0, 500 mM NaCl, 4°C). The following day, McbR was further purified using Ni-NTA (Qiagen) to isolate the cleaved protein from the TEV protease (itself His_6-tagged) and the cleaved His_6-tag. After concentration, McbR was purified in a final step using size exclusion chromatography (SEC; Superdex 200 26/60; 20 mM Tris pH 7.8, 100 mM NaCl, 0.5 mM TCEP). To determine the oligomerization state of McbR, the elution volume was compared to that of MW weight standards (BioRad).

Crystallization, data collection, and processing.

SeMet $McbR_{10-221}$ was concentrated to 8-10 mg/mL, incubated for 1 hr with glycerol (10% (v/v), final concentration) and used immediately for crystallization trials. Microcrystals of SeMet $McbR_{10-221}$ were obtained in 2 M sodium malonate pH 7.0 (sitting drop vapor diffusion; 25ºC) and used as seed solution to produce crystals in the same condition suitable for data collection. The crystals were cryo-protected in mother liquor containing 20% (v/v) MPD and immediately frozen in liquid nitrogen. Data for $McbR_{10-221}$ were collected at the National Synchrotron Light Source, beamline X25 using a Pilatus 6M detector (Dectris). Anomalous data was collected from a single crystal and phased using single anomalous dispersion (SAD) collecting data at 0.93 Å. Data were processed and scaled using HKL2000.[13] The asymmetric unit contains two protein molecules. The anomalous data was phased using HKL2MAP[14] (ShelxC/D/E);[15-17] 14 of the 16 expected selenium sites were identified. Approximately 90% of the structure was built automatically using ARP/wARP.[18] Model building and refinement of SeMet McbR was carried out using a high resolution dataset (2.1 Å) collected at 0.9793 Å. Iterative model building and refinement were performed using COOT[19] and *Phenix*.[20] The final model was refined with *Phenix* using TLS. Molprobity was used for model validation.[21] Analysis of the dimerization interface was performed using the Protein Interaction Calculator,[22] with solvent accessible surface areas calculated using Naccess.[23] Cavity volumes were calculated using POCOSA.[24] Data collection and structure refinement statistics are reported in **Table 1**.

Electrophoretic mobility shift assay.

The *E. coli yciG* promoter ($PyciG_{ECO}$) was used for DNA binding studies. Following synthesis of the individual oligonucleotides (IDT Technologies; each oligonucleotide includes a 3′ biotin label; **Table 2**), the complementary oligonucleotides were combined, heated to 95°C and then cooled by 1°C per min to a final temperature of 25°C. For EMSA experiments, 1 pmol

of protein was added to the biotin-labeled DNA (P*yciG*$_{ECO}$, 100 fmol). All reactions were carried out in binding buffer (10 mM Tris pH 7.5, 50 mM KCl, 1 mM DTT) in the presence of a poly (dI-dC) DNA probe (50 ng/μL) to prevent non-specific binding. For the unlabeled competitor EMSA control, a 200-fold excess of unlabeled P*yciG*$_{ECO}$ DNA was added. All binding reactions were incubated at room temperature for 20 min. Samples were then loaded onto a 6% DNA retardation gel (Invitrogen) and subjected to electrophoresis at 4°C for 75 min at 100 V in 0.5-fold TBE buffer (45 mM Tris pH 8.3, 45 mM Boric acid, 1 mM EDTA). The DNA was transferred to a nylon membrane at 390 mA for 30 min, followed by UV crosslinking at 302 nm by placing the membrane face-down on a UV illuminator for 15 min. Chemiluminescence was performed using the LightShift Chemiluminescent EMSA Kit (Pierce) and the samples were detected using a CCD imager (Typhoon 9410 Imager).

Mucoidy assay.

WT *mcbR* and two mutated *mcbR* variants (*mcbR*-E93S-R139F and *mcbR*-R89A-E93A-R139A) were subcloned from pRP1B-*mcbR*, pRP1B-*mcbR*-E93S-R139F, and pRP1B-*mcbR*-R89A-E93A-R139A into the *Kpn*I and *Sac*I sites of pBS(Kan)[25] using primers in **Table 3**, so that their expression is under control of a *lac* promoter (instead of a T7 promoter in the former plasmids). The resulting plasmids are pBS(Kan)-*mcbR*, pBS(Kan)-*mcbR*-E93S-R139F, and pBS(Kan)-*mcbR*-R89A-E93A-R139A. After verifying these plasmids by DNA sequencing, they were introduced into *E. coli* MG1655 Δ*mcbR* Δ*Km*[4] *via* electroporation, and the transformed clones were plated on LB agar supplemented with 50 μg/mL kanamycin and 0.2% (w/v) glucose. At least three independent colonies were streaked on LB agar supplemented with 50 μg/mL kanamycin and 1 mM IPTG to test the mucoidy of each strain. Cells were incubated at 37ºC for 12 h.

RESULTS AND DISCUSSION

McbR is a member of the VanR subfamily of GntR transcriptional regulators

Two constructs of McbR were screened for their ability to form diffraction quality crystals: $McbR_{1-221}$ and $McbR_{10-221.}$ The latter is missing the first 9 amino acids, which were predicted to be disordered (PSIPRED,[26] IUPRED[27, 28]). Only $McbR_{10-221}$ formed crystals suitable for structure determination and is referred to hereafter as McbR. The crystal structure of McbR was determined by single-wavelength anomalous dispersion (SAD) using SeMet-labeled protein and the atomic model was refined to 2.1 Å resolution (**Table 1; Fig. 1B; Fig. 2A**). Two molecules of McbR are present in the asymmetric unit and are related by a nearly perfect two-fold axis (179.8º; superposition using the C-terminal FCD domain; **Fig. 2A**). This is consistent with the observation that McbR is predominantly a dimer in solution (**Fig. 2B**). McbR, like other members of the GntR family, consists of an N-terminal wHTH domain (residues 10-76; residues 38-46 in the second subunit were not modeled due to a lack of clear electron density) and a C-terminal all α-helical effector-binding domain (residues 77-219; **Fig. 1B**). The wHTH domain is composed of three α-helices (α1-α3) and three β-strands (β1-β3), which form a small β-sheet that is a defining characteristic of the wHTH fold. The C-terminal domain is composed of six α-helices (α4-α9). The secondary structure elements and topology of the C-terminal domain places McbR in the FadR C-terminal domain (FCD) family of GntR transcriptional regulators (**Fig. 1A**).

McbR dimerization interface is extensive including both the N- and C-terminal domains

The FCD family has ~2800 members from more than 400 distinct species from archaea to eukaryota.[10] A structural homology search using Dali identified only 6 other structures that have a high degree of similarity to McbR (Z-score > 7 using only the FCD domain; **Table 4; Fig. 3**). These represent the only other members of the FCD family with known structures. The dimerization interface mediated by the C-terminal FCD domain is topologically conserved within the FCD family and is composed of the first helix in the FCD domain (α4 in McbR) and the N-terminal half of the kinked fourth helix (α7 in McbR). In McbR, the FCD dimerization interface buries 1655 Å^2 of solvent accessible surface area, which is 70% of the buried surface area (BSA) for the entire McbR dimer. The hydrophobic core of the FCD dimerization interface is formed by residues Ile85, Ile88, Leu92, Met148, Ile150, Leu151, Met154 and Leu158 from both monomers, each of which is completely occluded from solvent (**Fig. 2C**). It is further stabilized by polar and salt bridge interactions, especially a bidentate hydrogen bond between $Gln157_A$ and $Gln157_B$ and a bidentate salt bridge between $Arg161_A$ and $Glu153_B$ ('A' or 'B' subscript indicates the residue is from subunit 'A' or 'B', respectively; **Fig. 2D**).

In McbR, the wHTH domains also interact, extending the dimerization interface beyond that typically observed in the FCD subfamily of GntR regulators. The wHTH interface buries 740 Å^2 of BSA, for a total of 2395 Å^2 buried between the two McbR monomers. While the FCD domains are related by a near perfect two-fold axis centered on $Gln157_{A/B}$, the wHTH are not. Instead, they are related by a rotation of ~172º. Thus, while $Leu56_A$ is buried in the wHTH interface, the corresponding residue ($Leu56_B$) is located at the interface periphery (**Fig. 2E**). The wHTH dimerization is composed largely of polar interactions (i.e., a hydrogen bond between $Ser60_{A/B}$ and $Arg57_{A/B}$) and a few hydrophobic interactions ($Leu14_B$ and $Leu56_A$); however,

unlike the residues at the FCD interface, none of the wHTH interface residues become extensively buried upon complex formation (**Fig. 2E**). Finally, $Asn62_A$ (wHTH domain) hydrogen bonds with $Glu153_B$ (FCD domain); this is the only non-covalent interaction connecting the two different domains from the distinct subunits in the dimer.

Comparison of McbR with the other members of the FCD subfamily reveals that while the FCD dimerization interface is conserved within the family, the relative orientation of the wHTH and FCD domains is not. This gives rise to distinct differences in the orientations of the wHTH domains and, in some cases, distinct quaternary structures (**Fig. 3**). This is why the FCD family member identified to be most similar to McbR using the DALI structural homology search database changes depending on whether or not the search is performed with the McbR FCD domain alone (PS5454, PDBID 3C7J) or full-length McbR (REJMP134, PDBID 3IHU; **Table 4**). As expected, the FCD proteins identified as most different from full-length McbR are FadR and CGL2915. These are also both members of the FadR subfamily, but have an additional helix between the wHTH and the FCD ligand binding domains (**Fig. 4**). The presence of this helix leads to domain swapped quaternary structures, in which the wHTH domain of subunit 'A' crosses the dimerization interface to make contacts with the FCD domain of subunit 'B'. This domain swapping is not observed in the VanR subclass of FCD regulators and instead, in these proteins, the wHTH and FCD domains of the same subunit are more intimately associated.

The structure of McbR is predominantly in a ligand bound conformation

The C-terminal FCD domains are composed of either 6 (VanR subclass) or 7 (FadR subclass) α-helices which form an antiparallel helical bundle. McbR, which has 6 helices, is a

member of the VanR subclass (**Fig. 1A**). The FCD domains have a large cavity in the center of this helical bundle, which is the location of the ligand binding site. The structure of this cavity is identical between both FCD domains in McbR, as the FCD domains superimpose with a root mean square deviation (rsmd) of only 0.24 Å (**Fig. 6B**). Although the helical topology is conserved among FCD domains, the sequence conservation between FCD family members, especially the residues that line the ligand binding cavities, is very low, likely reflecting their distinct ligand specificities (**Fig. 4A**).

Recently it was shown that the majority of FCD family members use three conserved histidines to bind a metal ion in the ligand binding cavity, suggesting that these regulators bind ligands that interact directly with the bound metal (**Fig. 4A, B**).[10] In McbR, these histidines are not conserved and are instead replaced by Arg139, Tyr185 and Ile207 (**Fig. 4B**). Thus, McbR is one of the few FCD family members that does not bind a metal. Because of this, the ligand pocket in McbR is large, with a volume of ~200 $Å^3$, nearly double that of the metal-binding FCD domains (**Fig. 4C**). Although the endogenous ligand for McbR is still unknown, clear unambiguous density for a bound entity was observed in the FCD ligand binding cavities of both monomers of McbR (**Fig. 4D**). None of the protein and crystallization buffer components, or derivatives thereof, fit the density. This is likely because the density is rather undefined, potentially because it is not fully occupied, a phenomenon commonly observed without externally supplied ligands and/or cofactors. Alternatively, the density could correspond to the biologically relevant ligand, as McbR is an *E. coli* protein and was expressed in *E. coli*. However, potential ligands, such as gluocuronic acid, a component of colanic acid whose metabolism has been shown to be regulated by McbR, did not fit the density.[4] Finally, automated ligand fitting routines, such as the LigandFit program implemented in Phenix, also failed to

identify a ligand that satisfactorily fit the density.[29, 30] Because the density did not enable the identity of the ligand to be confidently determined, it has not been modeled.

However, the presence of the density did reveal the identity of the residues that likely define the McbR ligand binding site. Namely, the bound entity is strongly coordinated by two arginine residues, Arg89 and Arg139, which themselves are organized via a shared salt bridge with Glu93 (**Figs. 4C, D**). Two neighboring asparagine residues, Asn135 and Asn211, also contribute to binding. To investigate whether these residues are important for McbR function, we generated two variants of McbR by mutating the residues that define the entity binding site. Because mutating residues in the interior of a protein can also lead to protein unfolding, we generated two distinct mutants: a double mutant in which Glu93 and Arg139 were substituted with Ser and Phe respectively, the structurally homologous residues in FadR (the residue structurally homologous to McbR Arg89 is also an Arg in FadR) and a triple mutant in which all three residues were mutated to alanines (Arg89Ala, Glu93Ala and Arg139Ala). CD polarimetry demonstrated that both McbR variants are folded and EMSAs showed they are functional (**Fig. S1**). The mutants were somewhat less thermostable (ΔT_m of -8.6 C and -18.6 C, compared to wt for the double and triple mutant respectively), but this was expected as the mutations are in the interior of the protein; indeed, this is exactly why two mutants, one in which the residues were mutated to those present in FadR (the double mutant) and one in which the residues were simply mutated alanine (the triple mutant), were tested. McbR deletion from *E. coli* results in EPS overproduction and elicits a mucoidy phenotype.[4] This mucoidy phenotype is substantially reduced upon producing McbR ectopically (**Fig. 5**). However, cells producing McbR with triple mutations (Arg89Ala, Glu93Ala, Arg139Ala) are mucoid (**Fig. 5**). This observation demonstrates the importance of Arg89, Glu93, and Arg139 in binding the unknown ligand, and

more importantly, the physiological relevance of the unknown ligand in affecting EPS production. Both Arg89 and Arg139 are required for ligand binding, as cells producing McbR with only two mutations (Glu93Ser and Arg139Phe) also remain less mucoid than cells with empty plasmid or cells producing McbR with three mutations (Arg89Ala, Glu93Ala, Arg139Ala) (**Fig. 5**).

The conformation of McbR crystallized is likely incompatible with DNA binding

The wHTH domain is defined by helix α2, a connecting turn, and helix α3 ("HTH"), and a small loop in the anti-parallel β-sheet (the "wing"). The wHTH domain is slightly more conserved than the FCD domain (5% identity, 13% similar) when comparing the 7 structurally characterized FCD family members, with McbR residues Leu20, Leu24, Leu29, Gly32, Leu35, Leu40, Leu44, Met46, Val51, Arg52, Glu53, Leu55, Leu58, and Leu64 being highly similar (**Fig. 4A**). The conserved hydrophobic residues function to stabilize the wHTH domain fold, while the two charged residues are located at the wHTH dimerization interface (**Fig. 2E**).

In McbR, the C-terminal portion of wHTH helix α1 contributes to the 'top' of the FCD binding cavity, with Ile26 (helix α1) ~12 Å away from the FCD domain ligand coordinating arginines (Arg89 and Arg139; **Fig. 6A**). Thus, this wHTH-FCD interface provides a conduit by which effector binding in the FCD domain can be structurally communicated to wHTH DNA binding domain.[8] The conformation and orientation of the McbR wHTH domains appear to be incompatible with DNA binding. First, residues 37-48, which comprise helix α2 are disordered in subunit 'B' (**Fig. 2A**). Residues from helix α2 often contribute to DNA recognition, as has been observed for the FCD transcription factor FadR.[9] Second, the two domains in McbR differ

not only in their relative orientations to the FCD domain, but also in conformation, with an RMSD of 1.2 Å (**Fig. 6B**). This is due to a change in the orientation of the 'wing' between strands β2 and β3.

Implications for McbR function

Currently, *E. coli* FadR is the only member of the GntR family whose DNA-bound structure has been determined,[8, 9] revealing that FadR binds the short palindromic consensus sequence 5'-TGGNNNNNCCA-3'. Previously, the *E. coli* McbR protein was shown to bind upstream of the *E. coli yciGFE* promoter (P*yciG*$_{ECO}$).[6] Subsequent DNaseI footprinting identified two distinct DNA sequences within P*yciG*$_{ECO}$ protected by McbR binding. To confirm that McbR binds this operator, we performed EMSA experiments using wt McbR and P*yciG*$_{ECO}$ DNA. As shown in **Fig. 7**, McbR binds and shifts P*yciG*$_{ECO}$ DNA.

In the FadR:DNA complex, Arg35 (helix α2), Arg45 (helix α3), Thr46 (helix α3) and His65 (β2-β3 'wing') mediate base-specific contacts with the bound DNA. The corresponding residues in McbR are Lys38, Ile48, Thr49, respectively, with no residue corresponding to His65 (**Fig. 7A**). This suggests that McbR likely interacts with DNA via helix α2 (Lys38) and helix α3 (Thr46). Superposition of the FadR:DNA complex and McbR shows Gln70 as the only residue with a polar side chain in close proximity with the DNA in the β2-β3 'wing'. Additional basic residues in close proximity to the DNA include Arg34 and Arg52 (**Fig. 7A**). We tested the role of these residues in DNA binding using EMSA experiments performed with the P*yciG*$_{ECO}$ promoter DNA and McbR mutants (we used CD to show that the variants are folded; **Fig. S1**; the T_m's of the variants are within 3.7 ºC of wt, which has a T_m of 63.2 ºC). The EMSA experiments

show that residues Arg34, Lys38, Thr49 and Arg52 are important for DNA binding, as mutating these residues to alanine result in a loss of DNA binding compared to wild-type McbR (**Fig. 7B**). Furthermore, Arg34, Lys38, Thr49 have the most debilitating effects, suggesting that β1, α2 and α3 play key roles in DNA binding.

So how is DNA binding regulated? As stated earlier, the GntR transcription factors are typically regulated by ligands that are metabolic substrates/products/cofactors of the genes they regulate. In many cases, these genes are often located next to or near the GntR gene itself.[7] McbR was previously shown to bind the promoter of *yciGFE* and *ybiM*.[4, 6] While the molecular functions of the protein products of these genes are currently unknown, *ybiM* has been shown to effect colanic acid production in a McbR-dependent manner, suggesting that colonic acid, or one of its constituents, may be the biologically relevant ligand for McbR.[4] Currently, our results suggest that this is not the case, as none of the components of colanic acid satisfactorily fit the ligand density in the McbR cavity. An examination of the genes near *mcbR* in the *E. coli* chromosome shows that they are involved in a variety of biological processes (**Table 5)**; our data again shows that McbR is unlikely to be regulated by these metabolites (methionine, curcumin/dihydrocurcumin, iron, asparagine and glutathione) as they also did not satisfactorily fit the density. However, sequence similarities between the *E. coli* and *Samonella* McbR do suggest that they likely bind similar, if not identical, ligands. Namely, while the FCD domains of McbR from both organisms are less conserved that their corresponding wHTH domains (FCD domain sequence conservation: 46% identity, 74% similarity), the ligand binding residues are nearly perfectly conserved, including Arg89, Glu93 and Arg139 (**Fig. 4A**); the only differences in the ligand binding pocket are distal from the Arg-Glu-Arg pocket: Ile214 and Leu215 (Thr214 and Thr215 in *Samonella*). Because these residues change from hydrophobic (*E. coli*) to polar

(*Samonella*), the distal portion of the ligand may be slightly different between the organisms. Once the biologically relevant ligand(s) of McbR have been confidently identified, this ligand, or a derivative thereof, may be able to function as a novel therapeutic to target biofilms.

ACKNOWLEDGMENT

Data for this study were measured at beamline X25 of the National Synchrotron Light Source (supported principally by the Offices of Biological and Environmental Research and of Basic Energy Sciences of the United States Department of Energy and by the National Center for Research Resources of the National Institutes of Health). This research is based in part upon work conducted in the Center for Genomics and Proteomics Core Facility (with partial support from the National Institutes of Health, NCRR Grants P30RR031153, P20RR018728, and S10RR02763, National Science Foundation-EPSCoR Grant 0554548, Lifespan Rhode Island Hospital, and the Division of Biology and Medicine, Brown University) and also in the Rhode Island NSF/EPSCoR Proteomics Share Resource Facility (supported in part by the National Science Foundation EPSCoR Grant No. 1004057, National Institutes of Health Grant No. 1S10RR020923, S10RR027027, a Rhode Island Science and Technology Advisory Council grant, and the Division of Biology and Medicine, Brown University).

SUPPORTING INFORMATION

CD spectra and EMSA of McbR variants (Figure S1). This material is available free of charge via the Internet at http://pubs.acs.org

REFERENCES

1. Lewis, K. (2001) Riddle of biofilm resistance, *Antimicrobial agents and chemotherapy 45*, 999-1007.
2. Potera, C. (1999) Forging a link between biofilms and disease, *Science 283*, 1837, 1839.
3. Spoering, A. L., and Lewis, K. (2001) Biofilms and planktonic cells of Pseudomonas aeruginosa have similar resistance to killing by antimicrobials, *Journal of bacteriology 183*, 6746-6751.
4. Zhang, X. S., Garcia-Contreras, R., and Wood, T. K. (2008) Escherichia coli transcription factor YncC (McbR) regulates colanic acid and biofilm formation by repressing expression of periplasmic protein YbiM (McbA), *The ISME journal 2*, 615-631.
5. Whitfield, C. (2006) Biosynthesis and assembly of capsular polysaccharides in Escherichia coli, *Annual review of biochemistry 75*, 39-68.
6. Beraud, M., Kolb, A., Monteil, V., D'Alayer, J., and Norel, F. (2010) A proteomic analysis reveals differential regulation of the sigma(S)-dependent yciGFE(katN) locus by YncC and H-NS in Salmonella and Escherichia coli K-12, *Molecular & cellular proteomics : MCP 9*, 2601-2616.
7. Hoskisson, P. A., and Rigali, S. (2009) Chapter 1: Variation in form and function the helix-turn-helix regulators of the GntR superfamily, *Advances in applied microbiology 69*, 1-22.
8. van Aalten, D. M., DiRusso, C. C., Knudsen, J., and Wierenga, R. K. (2000) Crystal structure of FadR, a fatty acid-responsive transcription factor with a novel acyl coenzyme A-binding fold, *The EMBO journal 19*, 5167-5177.
9. Xu, Y., Heath, R. J., Li, Z., Rock, C. O., and White, S. W. (2001) The FadR.DNA complex. Transcriptional control of fatty acid metabolism in Escherichia coli, *The Journal of biological chemistry 276*, 17373-17379.
10. Zheng, M., Cooper, D. R., Grossoehme, N. E., Yu, M., Hung, L. W., Cieslik, M., Derewenda, U., Lesley, S. A., Wilson, I. A., Giedroc, D. P., and Derewenda, Z. S. (2009) Structure of Thermotoga maritima TM0439: implications for the mechanism of bacterial GntR transcription regulators with Zn2+-binding FCD domains, *Acta crystallographica. Section D, Biological crystallography 65*, 356-365.
11. Peti, W., and Page, R. (2007) Strategies to maximize heterologous protein expression in Escherichia coli with minimal cost, *Protein expression and purification 51*, 1-10.
12. Brown, B. L., Grigoriu, S., Kim, Y., Arruda, J. M., Davenport, A., Wood, T. K., Peti, W., and Page, R. (2009) Three dimensional structure of the MqsR:MqsA complex: a novel TA pair comprised of a toxin homologous to RelE and an antitoxin with unique properties, *PLoS pathogens 5*, e1000706.
13. Otwinowski, Z., and Minor, W. (1997) Processing of X-ray diffraction data collected in oscillation mode, *Method Enzymol 276*, 307-326.
14. Pape, T., and Schneider, T. R. (2004) HKL2MAP: a graphical user interfact for macromolecular phasing with SHELX programs, *Appl Cryst 37*, 843-844.
15. Schnieider, T. R., and Sheldrick, G. M. (2002) Substructure solution with SHELXD, *Acta crystallographica. Section D, Biological crystallography 58*, 1772-1779.
16. Sheldrick, G. M. (2002) Macrmolecular phasing with SHELXE, *Z. Kristallogr. 217*, 664-650.
17. Sheldrick, G. M. (2003) SHELXC, Goettingen University.

18. Langer, G., Cohen, S. X., Lamzin, V. S., and Perrakis, A. (2008) Automated macromolecular model building for X-ray crystallography using ARP/wARP version 7, *Nature protocols 3*, 1171-1179.
19. Emsley, P., Lohkamp, B., Scott, W. G., and Cowtan, K. (2010) Features and development of Coot, *Acta crystallographica. Section D, Biological crystallography 66*, 486-501.
20. Adams, P. D., Afonine, P. V., Bunkoczi, G., Chen, V. B., Davis, I. W., Echols, N., Headd, J. J., Hung, L. W., Kapral, G. J., Grosse-Kunstleve, R. W., McCoy, A. J., Moriarty, N. W., Oeffner, R., Read, R. J., Richardson, D. C., Richardson, J. S., Terwilliger, T. C., and Zwart, P. H. (2010) PHENIX: a comprehensive Python-based system for macromolecular structure solution, *Acta crystallographica. Section D, Biological crystallography 66*, 213-221.
21. Chen, V. B., Arendall, W. B., 3rd, Headd, J. J., Keedy, D. A., Immormino, R. M., Kapral, G. J., Murray, L. W., Richardson, J. S., and Richardson, D. C. (2010) MolProbity: all-atom structure validation for macromolecular crystallography, *Acta crystallographica. Section D, Biological crystallography 66*, 12-21.
22. Tina, K. G., Bhadra, R., and Srinivasan, N. (2007) PIC: Protein Interactions Calculator, *Nucleic acids research 35*, W473-476.
23. Hubbard, S. J., and Thornton, J. M. (1993) NACCESS, p Computer Program, http://www.bioinf.manchester.ac.uk/naccess/.
24. Yu, J., Zhou, Y., Tanaka, I., and Yao, M. (2010) Roll: a new algorithm for the detection of protein pockets and cavities with a rolling probe sphere, *Bioinformatics 26*, 46-52.
25. Canada, K. A., Iwashita, S., Shim, H., and Wood, T. K. (2002) Directed evolution of toluene ortho-monooxygenase for enhanced 1-naphthol synthesis and chlorinated ethene degradation, *Journal of bacteriology 184*, 344-349.
26. Buchan, D. W., Minneci, F., Nugent, T. C., Bryson, K., and Jones, D. T. (2013) Scalable web services for the PSIPRED Protein Analysis Workbench, *Nucleic acids research 41*, W349-357.
27. Dosztanyi, Z., Csizmok, V., Tompa, P., and Simon, I. (2005) IUPred: web server for the prediction of intrinsically unstructured regions of proteins based on estimated energy content, *Bioinformatics 21*, 3433-3434.
28. Dosztanyi, Z., Csizmok, V., Tompa, P., and Simon, I. (2005) The pairwise energy content estimated from amino acid composition discriminates between folded and intrinsically unstructured proteins, *Journal of molecular biology 347*, 827-839.
29. Terwilliger, T. C., Adams, P. D., Moriarty, N. W., and Cohn, J. D. (2007) Ligand identification using electron-density map correlations, *Acta crystallographica. Section D, Biological crystallography 63*, 101-107.
30. Terwilliger, T. C., Klei, H., Adams, P. D., Moriarty, N. W., and Cohn, J. D. (2006) Automated ligand fitting by core-fragment fitting and extension into density, *Acta crystallographica. Section D, Biological crystallography 62*, 915-922.

Table 1. Crystallographic data collection and refinement statistics

Crystal data		
Space Group	$P6_3$	
No. McbR/ASU	2	
a, c [Å]	a=107.6, c=72.7	
Data Collection		
Wavelength (Å)	0.9793	0.9300
Unique Reflections	28120	50871
Resolution (Å)*	50.0-2.1 (2.14-2.10)	50.0-2.15 (2.19-2.15)
Mean I/σ	18.1 (3.0)	18.4 (2.5)
Completeness (%)	100.0 (100.0)	99.3 (98.7)
Redundancy	9.8 (10.0)	5.1 (5.2)
R_{merge} (%)†	8.3 (55.8)	6.1 (45.4)
Refinement		
R_{work} (%)	16.8	
R_{free} (%)º	20.8	
No. non-hydrogen atoms	3214	
No. water molecules	163	
Ave. B-factor (Å^2)		
protein	43.6	
waters	43.4	
r.m.s.d. bond length (Å)	0.008	
r.m.s.d. bond angle (°)	1.003	
Ramachandran Plot		
Favored (%)	99.8	
Allowed (%)	100.0	
Disallowed (%)	0	
PDBID Code	4P9F	

*Highest resolution shell data are shown in parentheses. º5% of the reflections used for R_{free}.$^{\dagger}R_{merge}$ = $\Sigma_{hkl}\Sigma_i$ $|I_i(hkl)$ - $\langle I(hkl)\rangle|$ / $\Sigma_{hkl}\Sigma_i I_i(hkl)$ where $I_i(hkl)$ is the i^{th} observation of a symmetry equivalent reflection hkl. Reported values for the 0.93 Å dataset are for unmerged Friedel pairs.

Table 2. PCR primers used to generate P*yciG*$_{ECO}$ for EMSA experiments. F indicates forward primer and R indicates reverse primer.

Primer Name	Sequence (5' - 3')
P*yciG*$_{ECO}$-*F**	AATTGTTAATATATCCAGAATGTTCCTCAAAATATATTTTCCCTCTAT
P*yciG*$_{ECO}$-*R**	ATAGAGGGAAAATATATTTTGAGGAACATT CTGGATATATTAACAATT

**primer contains a 3' biotin label*

Table 3. Primers used to subclone *mcbR* variants into pBS(Kan) plasmids. F indicates forward primer and R indicates reverse primer.

Primer Name	Sequence (5' - 3')
mcbR-F	TTTGTTTGGTACCAAGAAGGAGATATACCATGGGCTCTG
mcbR-R	GCCGCAAGAGCTCATTAACGATTGTATTGCTGG

Table 4. FCD family members and their structural similarity to McbR.

Name	PDB	FCD only			Full-Length				Sub-family	Metal Binding	FCD Ligands*
		R	*Z*	*RMSD (Å)*	*R*	*Z*	*RMSD (Å)*	Id (%)			
McbR	4P9F	-	-	-	-	-	-	-	VanR	No	UNK
PS5454	3C7J	1	18.2	1.9	3	18.3	1.9	23	VanR	Yes	Ni
CGL2915	2DI3	2	15.5	2.6	5	15.5	4.0	20	FadR	Yes	Zn
RO03477	2HS5	3	15.4	2.6	2	19.7	3.1	19	VanR	No	Act
Reut_B4629	3IHU	4	15.4	2.5	1	20.3	2.6	16	VanR	No	-
TM0439	3FMS	5	14.8	2.4	4	16.6	3.1	22	VanR	Yes	Act, Ni
FadR	1H9G	6	12.8	2.6	6	12.6	6.2	14	FadR	No	CoA-Myr

*Ligands/metals bound at the ligand binding pocket; UNK, unknown; Act, acetate ion.
R, Z-score rank
Z, DALI Z-score
RMSD, root mean square deviation reported by DALI
Id, % sequence identity

Table 5. DNA sequences surrounding the *mcbR* (*yncC)* gene in *Escherichia coli* (MG1655).

Gene	Other Names	Gene Description
yncA	*mnaT, b1448*	Methionine N-acyltransferase; L-amino acid N-acyltransferase
yncB	*curA, b1449*	Curcumin/dihydrocurcumin reductase, NADPH-dependent
yncD	*b1451*	Predicted iron outer membrane transporter
yncE	*b1452*	ATP-binding protein, periplasmic, function unknown
yncF	*ansP, b1453*	L-asparagine transporter
yncG	*b1454*	Glutathione S-transferase homolog
yncH	*b1455*	Conserved protein, function unknown

Figure Legends

Figure 1. McbR classification and structure. A. Flowchart illustrating the classification of McbR within the GntR superfamily. **B.** McbR monomer with all secondary structural elements annotated. The N-terminal winged helix-turn-helix (wHTH) domain is shown in light blue and the C-terminal FCD domain is shown in teal; the 'wing' loop of the wHTH domain is labeled. McbR residues 10-220 were observed in the electron density maps for subunit 'A'.

Figure 2. Dimerization interface of McbR. A. McbR dimer, with one monomer colored in shades of blue and the second colored in shades of green. The N-terminal wHTH domains are colored in light blue and light green while the C-terminal FCD domains are colored in teal and dark green. The residues between β1/α3 of monomer 'B' are disordered and represented as a dotted line. The pseudo two-fold axis is indicated by an arrow. **B.** Size exclusion chromatogram of McbR with elution volumes of MW standards indicated (BioRad; calculated molecular weight of the McbR monomer is ~24.5 kDa). **C.** Hydrophobic interactions that stabilize the FCD domain dimerization interface; the pseudo 2-fold axis is indicated by a black circle. **D.** Polar/salt bridge interactions (shown as black dashed lines) that stabilize the FCD domain dimerization interface. **E**. Interactions at the wHTH domain interface (polar/salt bridge interactions shown as black dashed lines); Leu56 is labeled in italics to highlight that while $L56_A$ (light blue) is buried in the interface, $Leu56_B$ (bright green) is not and instead at the interface periphery.

Figure 3. Quaternary structures of FCD family. FCD family members whose structures have been determined are shown, with one monomer depicted in teal and one in gold. Metals bound to

the FCD domains are depicted as light blue spheres. Ligands/molecules bound in the FCD ligand binding pockets are shown as magenta spheres or sticks. The dimerization helices (α4 and α7 in McbR) are colored green and orange. The corresponding quaternary structures are depicted as cartoons, with the N-terminal domains shown as triangles and the C-terminal domains as spheres. **A.** Head-to-head dimerization in which both the wHTH domains and the FCD domains contribute to the dimerization interface. **B.** Dimerization in which the wHTH domains do not interact with either one another or the FCD domains. **C.** Head-to-head dimerization in which only the FCD domains contribute to the dimerization **D.** 'Domain swapping' dimerization in which the wHTH domain of one monomer reaches across the FCD domain interface to interact with the FCD domain of the second monomer. **E.** Same as D except the wHTH domains are inverted with respect to one another.

Figure 4. Ligand binding cavity of McbR and comparison to structural homologues. A. Multiple sequence alignment showing high conservation at the N-terminal domain (α1-β3) and the C-terminal domain (α4-α9) in McbR in comparison to the FCD family. Identical amino acids are highlighted in black and similar amino acids are highlighted in gray. $McbR_e$ represents *E. coli* McbR and $McbR_s$ represents *S. Typhimurium* McbR. Alpha helices are depicted as cylinders above the sequence alignment and the beta-strands as arrows. Asterisks mark the residues in FadR which make base-specific contacts with DNA. Residues that define the McbR ligand binding site are highlighted in yellow. Residues important for metal binding in the FCD family are highlighted in orange. **B.** Structural superposition of the three conserved histidines in metal binding FCD family members and the corresponding residues in McbR (teal). *Pseudomonas syringae* PS5454 (PDBID: 3C7J) is shown in green, *Thermotoga maritima* TM0439 (PDBID:

3FMS) is shown in orange, and *Cornybacterium glutamicum* LldR (PDBID: 2DI3) is shown in maroon. Each respective metal is shown as a sphere in the same color. **C.** *Left,* Cartoon depiction of McbR with the ligand binding cavities represented as purple surfaces. *Right,* enlarged image of the binding cavity highlighting the three conserved residues in McbR that appear to be important for ligand binding (colored as in the left panel). **D.** Electron density for the ligand binding cavity in chain A of McbR. Positive density is shown as green chicken wire. Residues coordinated the unidentified entity (see text) are shown as teal sticks. Sigma level for the $2F_o$-F_c map is 1.0. Sigma level for the F_o-F_c map is 3.0.

Figure 5. Mucoidy level of *E. coli* MG1655 Δ*mcbR* Δ*Km* producing different McbR variants. Each strain was grown on LB agar supplemented with 50 μg/mL kanamycin and 1 mM IPTG at 37ºC for 12 h. WT/Empty: *E. coli* MG1655/pBS(Kan), Δ*mcbR*/Empty: *E. coli* MG1655 Δ*mcbR* Δ*Km*/pBS(Kan), Δ*mcbR*/mcbR: *E. coli* MG1655 Δ*mcbR* Δ*Km*/pBS(Kan)-*mcbR*, Δ*mcbR*/E93S-R139F: *E. coli* MG1655 Δ*mcbR* Δ*Km*/pBS(Kan)-*mcbR*-E93S-R139F, Δ*mcbR*/R89A-E93A-R139A: *E. coli* MG1655 Δ*mcbR* Δ*Km*/pBS(Kan)-*mcbR*-R89A-E93A-R139A.

Figure 6. N-terminal domain of McbR. A. The 'pocket' of α1 into the FCD domain. Helices α6 and α7 are colored teal (cartoon), while helix α1 is shown in light blue (sticks). **B.** Superposition of McbR chain A (light blue/deep teal) and McbR chain B (light green/dark green). While the C-terminal domains superimpose well (deep teal/dark green), the N-terminal domains (light blue/light green) do not.

Figure 7. McbR:P*yciG*$_{ECO}$ EMSA experiments. A. Superposition of the N-terminal domain of McbR (teal) and *E. coli* FadR (beige, PDBID: 1HW2) bound to DNA. Residues making base specific contacts in FadR and the structurally overlapping residues in McbR are shown as sticks and labeled. **B.** EMSA experiments using biotin-labeled P*yciG*$_{ECO}$ and WT McbR (the migration of the DNA alone is shown in the left lane). **C.** EMSA experiments using biotin-labeled P*yciG*$_{ECO}$ and either WT McbR or the McbR variants as indicated; the migration of the DNA alone is shown in the left lane. All binding reactions in B and C contain the nonspecific poly(dI-dC) probe.

Figure 1

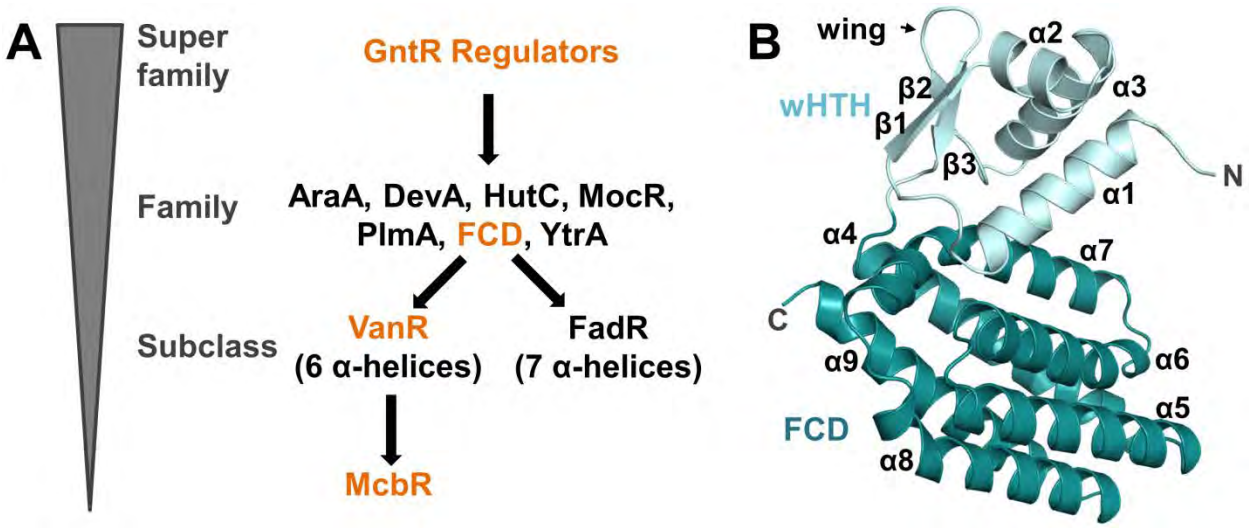
A
Super family
Family
Subclass
GntR Regulators
AraA, DevA, HutC, MocR, PlmA, FCD, YtrA
VanR (6 α-helices)
FadR (7 α-helices)
McbR
B
wing
α2
β2
α3
wHTH
β1
β3
N
α1
α4
α7
C
α9
α6
α5
FCD
α8

Figure 2

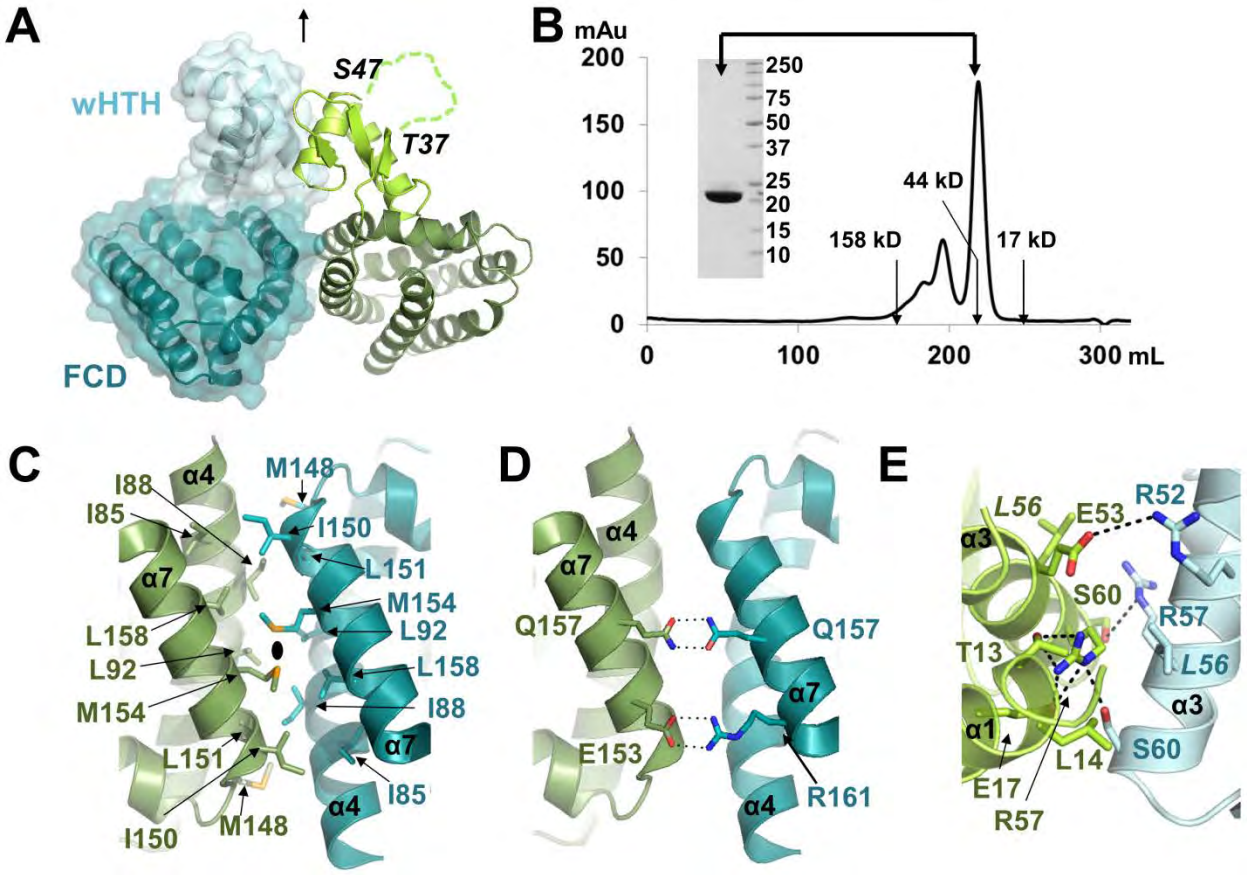
A
wHTH
S47
T37
FCD
B
mAu
200
150
100
50
0
250
75
50
37
25
20
15
10
44 kD
158 kD
17 kD
0
100
200
300 mL
C
I88
α4
M148
I85
I150
L151
α7
M154
L158
L92
L92
L158
M154
I88
α7
L151
I85
α4
I150
M148
D
α4
α7
Q157
Q157
α7
E153
R161
α4
E
L56
E53
R52
α3
S60
R57
T13
L56
α3
α1
S60
L14
E17
R57

Figure 3

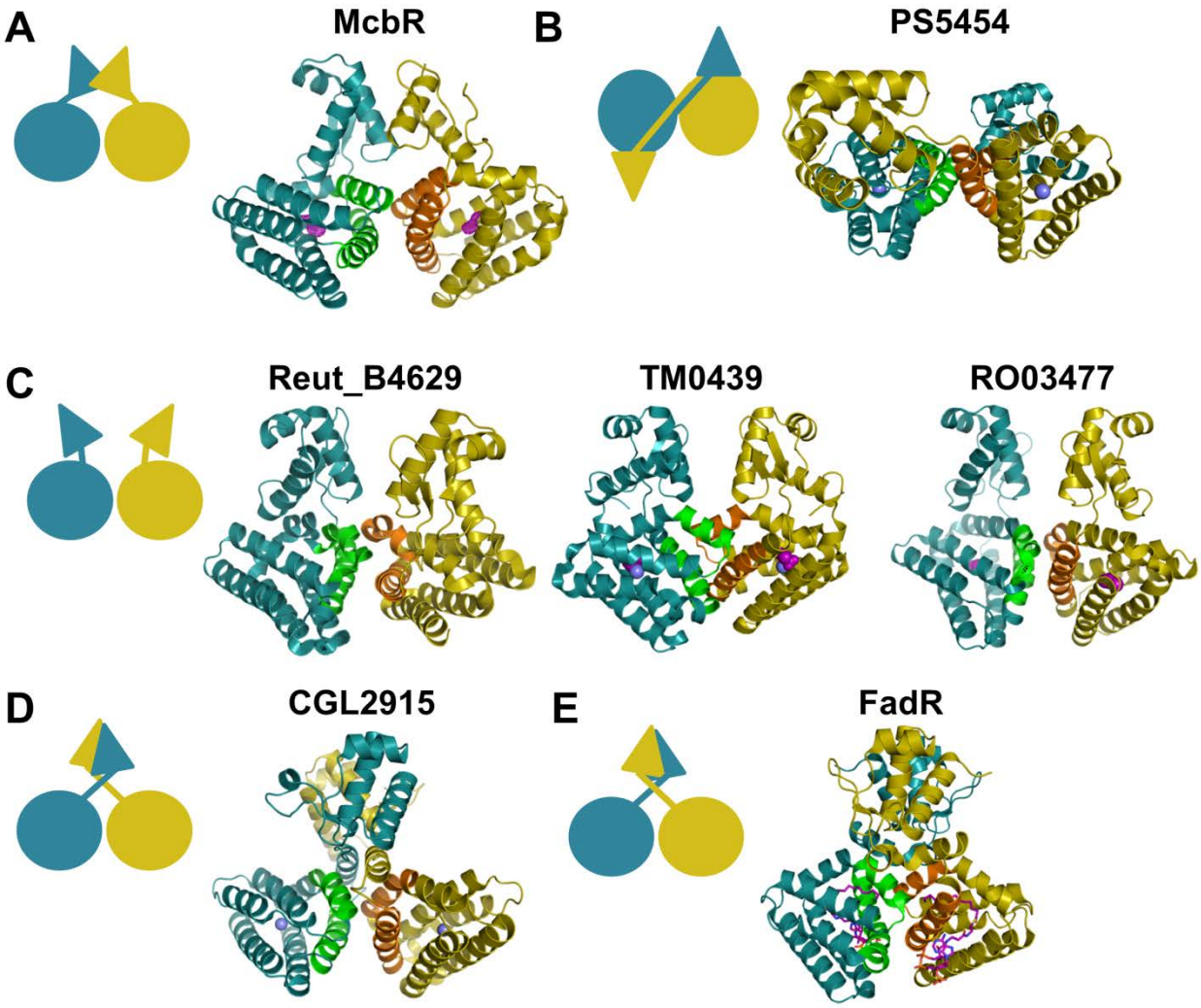

Figure 4

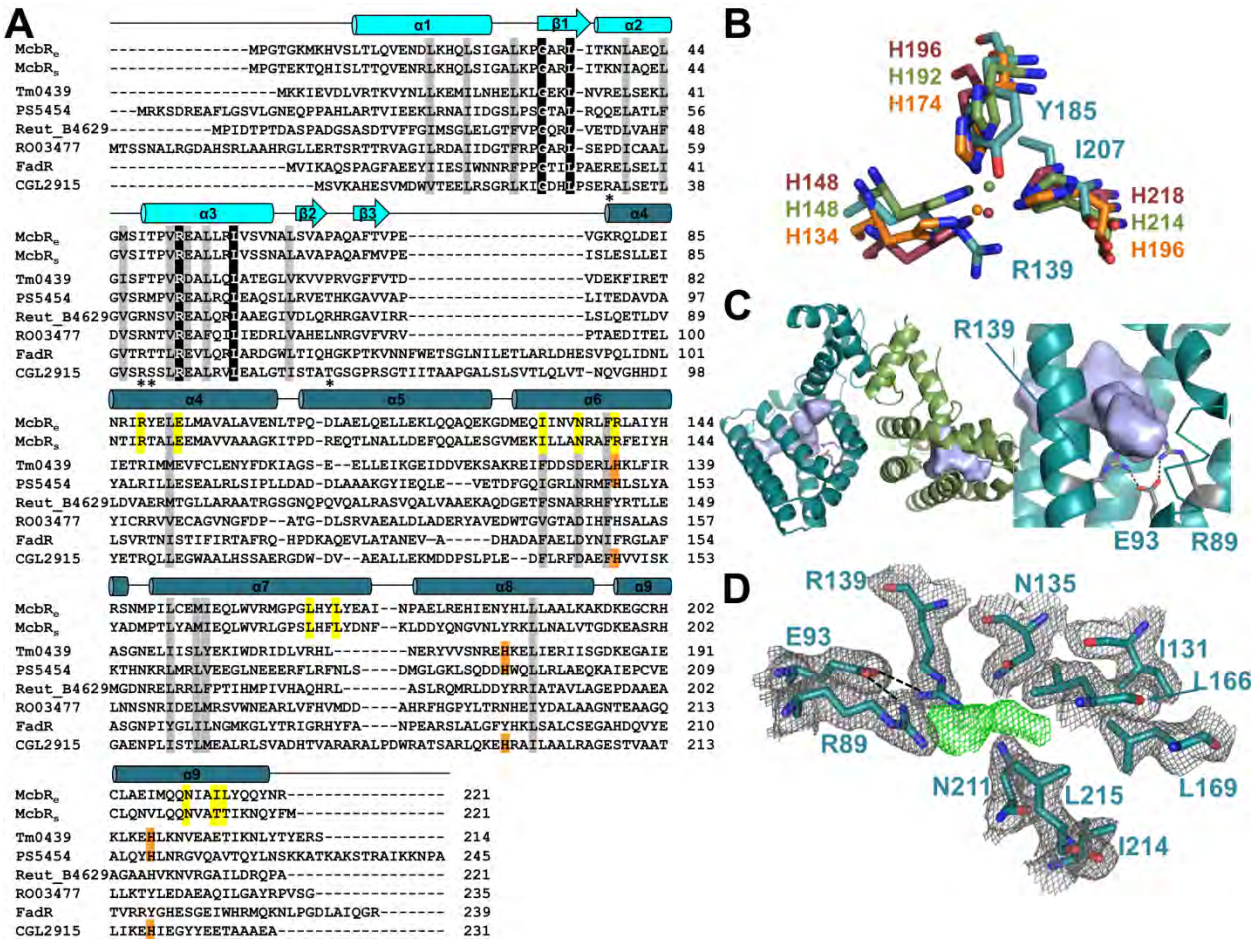
A
α1
β1
α2
McbR$_e$ ----------MPGTGKMKHVSLTLQVENDLKHQLSIGALKPGARL-ITKNLAEQL 44
McbR$_s$ ----------MPGTEKTQHISLTTQVENRLKHQLSIGALKPGARL-ITKNIAQEL 44
Tm0439 ----------MKKIEVDLVRTKVYNLLKEMILNHELKLGEKL-NVRELSEKL 41
PS5454 ---MRKSDREAFLGSVLGNEQPPAHLARTVIEEKLRNAIIDGSLPSGTAL-RQQELATLF 56
Reut_B4629----------MPIDTPTDASPADGSASDTVFFGIMSGLELGTFVPGQRL-VETDLVAHF 48
RO03477 MTSSNALRGDAHSRLAAHRGLLERTSRTTRVAGILRDAIIDGTFRPGARL-SEPDICAAL 59
FadR ----------MVIKAQSPAGFAEEYIIESIWNNRFPPGTIL-PAERELSELI 41
CGL2915 ----------MSVKAHESVMDWVTEELRSGRLKIGDHL-PSERALSETL 38
α3
β2
β3
α4
McbR$_e$ GMSITPVREALLRLVSVNALSVAPAQAFTVPE----------VGKRQLDEI 85
McbR$_s$ GVSITPVREALLRIVSSNALAVAPAQAFMVPE----------ISLESLLEI 85
Tm0439 GISFTPVRDALLQIATEGLVKVVPRVGFFVTD----------VDEKFIRET 82
PS5454 GVSRMPVREALRQIEAQSLLRVETHKGAVVAP----------LITEDAVDA 97
Reut_B4629GVGRNSVREALQRIAAEGIVDLQRHRGAVIRR----------LSLQETLDV 89
RO03477 DVSRNTVREAFQILIEDRLVAHELNRGVFVRV----------PTAEDITEL 100
FadR GVTRTTLREVLQRIARDGWLTIQHGKPTKVNNFWETSGLNILETLARLDHESVPQLIDNL 101
CGL2915 GVSRSSLREALRVIEALGTISTATGSGPRSGTIITAAPGALSLSVTLQLVT-NQVGHHDI 98
α4
α5
α6
McbR$_e$ NRIRYELELMAVALAVENLTPQ-DLAELQELLEKLQQAQEKGDMEQIINVNRLFRLAIYH 144
McbR$_s$ NTIRTALEEMAVVAAAGKITPD-REQTLNALLDEFQQALESGVMEKILLANRAFRFEIYH 144
Tm0439 IETRIMMEVFCLENYFDKIAGS-E--ELLEIKGEIDDVEKSAKREIFDDSDERLHKLFIR 139
PS5454 YALRILLESEALRLSIPLLDAD-DLAAAKGYIEQLE---VETDFGQIGRLNRMFHLSLYA 153
Reut_B4629LDVAERMTGLLARAATRGSGNQPQVQALRASVQALVAAEKAQDGETFSNARRHFYRTLLE 149
RO03477 YICRRVVECAGVNGFDP--ATG-DLSRVAEALDLADERYAVEDWTGVGTADIHFHSALAS 157
FadR LSVRTNISTIFIRTAFRQ-HPDKAQEVLATANEV-A-----DHADAFAELDYNIFRGLAF 154
CGL2915 YETRQLLEGWAALHSSAERGDW-DV--AEALLEKMDDPSLPLE--DFLRFDAEFHVVISK 153
α7
α8
α9
McbR$_e$ RSNMPILCEMIEQLWVRMGPGLHYLYEAI--NPAELREHIENYHLLLAALKAKDKEGCRH 202
McbR$_s$ YADMPTLYAMIEQLWVRLGPSLHFLYDNF--KLDDYQNGVNLYRKLLNALVTGDKEASRH 202
Tm0439 ASGNELIISLYEKIWDRIDLVRHL--------NERYVVSNREHKELIERIISGDKEGAIE 191
PS5454 KTHNKRLMRLVEEGLNEEEERFLRFNLS----DMGLGKLSQDDHWQLLRLAEQKAIEPCVE 209
Reut_B4629MGDNRELRRLFPTIHMPIVHAQHRL-------ASLRQMRLDDYRRIATAVLAGEPDAAEA 202
RO03477 LNNSNRIDELMRSVWNEARLVFHVMDD----AHRFHGPYLTRNHEIYDALAAGNTEAAGQ 213
FadR ASGNPIYGLILNGMKGLYTRIGRHYFA----NPEARSLALGFYHKLSALCSEGAHDQVYE 210
CGL2915 GAENPLISTLMEALRLSVADHTVARARALPDWRATSARLQKEHRAILAALRAGESTVAAT 213
α9
McbR$_e$ CLAEIMQQNIAILYQQYNR---------- 221
McbR$_s$ CLQNVLQQNVATTIKNQYFM---------- 221
Tm0439 KLKEHLKNVEAETIKNLYTYERS---------- 214
PS5454 ALQYHLNRGVQAVTQYLNSKKATKAKSTRAIKKNPA 245
Reut_B4629AGAAHVKNVRGAILDRQPA---------- 221
RO03477 LLKTYLEDAEAQILGAYRPVSG---------- 235
FadR TVRRYGHESGEIWHRMQKNLPGDLAIQGR------- 239
CGL2915 LIKEHIEGYYEETAAAEA---------- 231
B
H196
H192
H174
Y185
I207
H148
H148
H134
H218
H214
H196
R139
C
R139
E93
R89
D
R139
N135
E93
I131
L166
R89
N211
L215
L169
I214

Figure 5

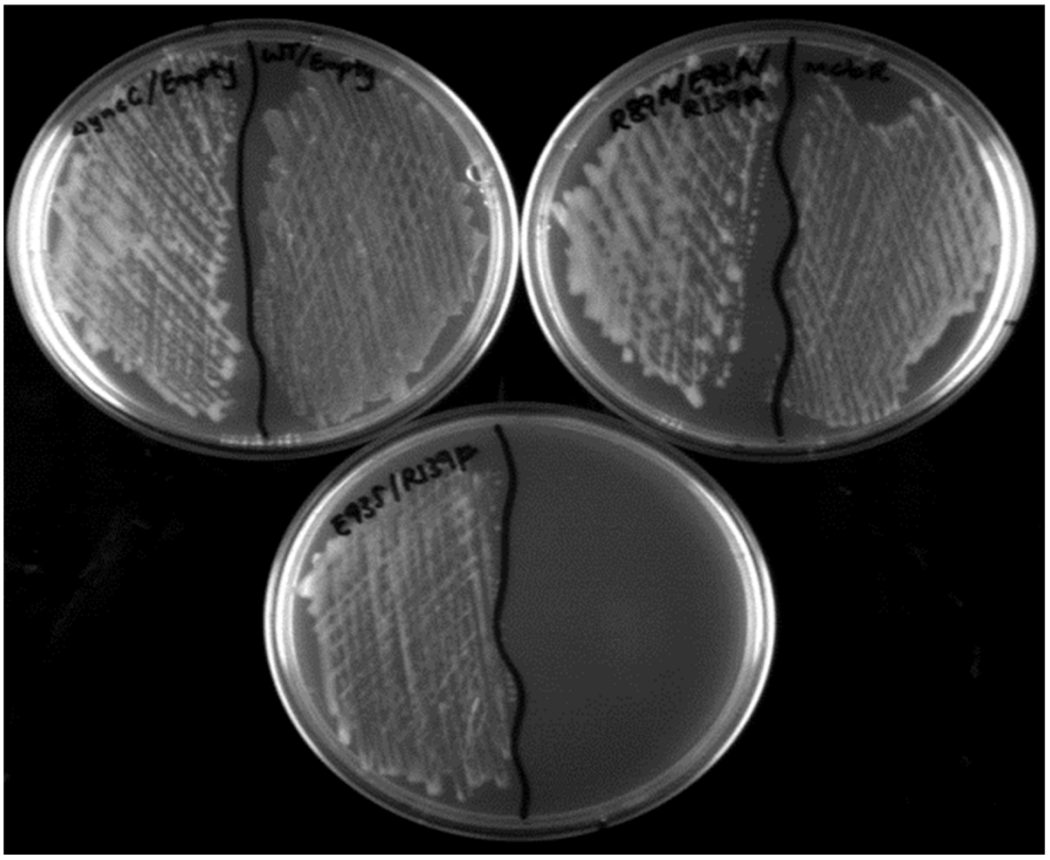

Figure 6

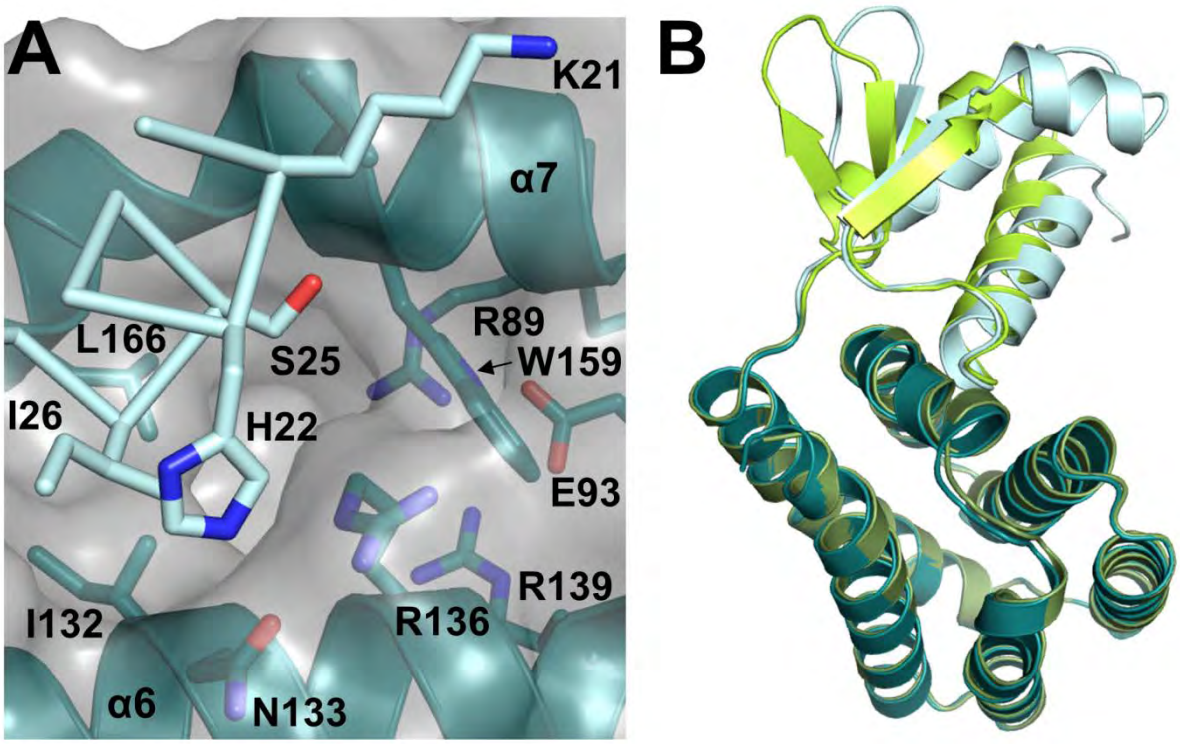

Figure 7

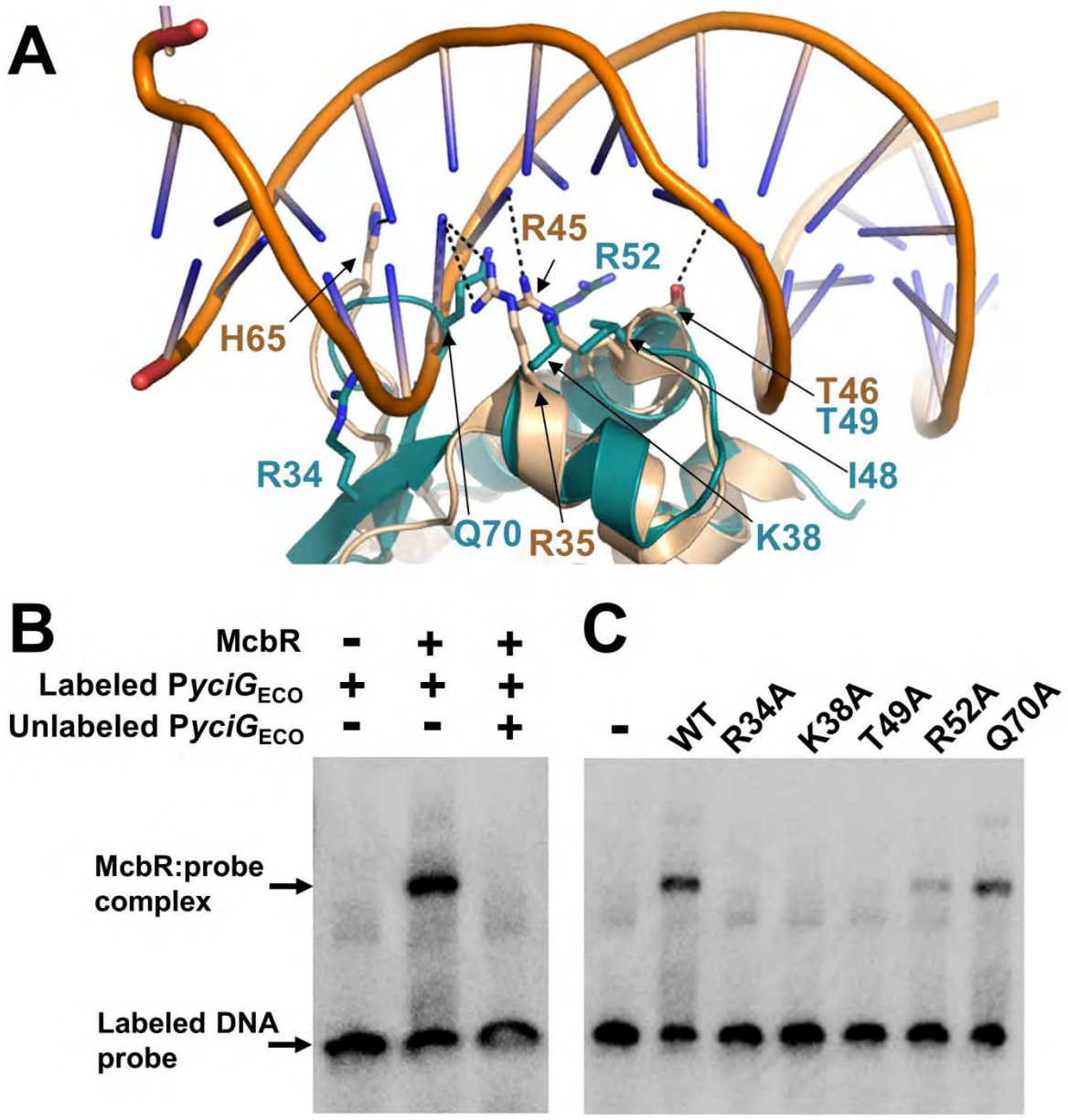
A
R45
R52
H65
T46
T49
I48
R34
Q70
R35
K38
B
McbR - + +
Labeled P*yciG*ECO + + +
Unlabeled P*yciG*ECO - - +
McbR:probe complex
Labeled DNA probe
C
-
WT
R34A
K38A
T49A
R52A
Q70A

TOC